Effective Rate Evaluation with Assistance of MG, MoG, and Fox's H-Function Distributions

Long Kong[†], Jiguang He[♭], Yun Ai[‡], Symeon Chatzinotas[†], and Björn Ottersten[†]

[†]The Interdisciplinary Centre for Security Reliability and Trust (SnT), University of Luxembourg, Luxembourg
[♭] Center for Wireless Communications (CWC), University of Oulu, Oulu, Finland
[‡]Faculty of Engineering, Norwegian University of Science and Technology, 2815 Gjøvik, Norway
Emails: long.kong@uni.lu, jiguang.he@oulu.fi, yun.ai@ntnu.no, symeon.chatzinotas@uni.lu, bjorn.ottersten@uni.lu

***Abstract*—This paper investigates the effective rate when the instantaneous received signal-to-noise ratio (SNR) could be modeled as the mixture Gamma (MG), mixture of Gaussian (MoG), and Fox's H-function distributed random variable (RV), respectively. Three closed-form expressions are correspondingly derived in terms of the Fox's H-function. The obtained analytical results are further examined by the Monte-Carlo simulation. One can observe that (i) the analytical solutions provide an excellent match with the Monte-Carlo simulation results; (ii) the MG and MoG approaches provide highly approximated solutions, and the MG is better due to a simpler form; and (iii) the Fox's H-function solution is exact and offers a unified, general and flexible framework for the effective rate analysis.**

***Index Terms*—Effective Rate, quality-of-service (QoS), mixture gamma (MG) distribution, mixture of Gaussian (MoG) distribution, Fox's H-function distribution.**

I. Introduction

Future generation of communication systems are bound to change the landscape of industry thanks to the Industrial Internet of Things (IIoT) enabled by extreme low latency and massive number of connections. Due to the highly time-varying characteristics of the wireless channel, deterministic delay constraints are normally difficult to meet. Instead, the statistical quality-of-service (QoS) provisioning turns out to be a useful instrument to evaluate the delay bound QoS guarantees for realistic wireless real-time traffic.

In this context, the effective rate serves a statistical QoS metric defined as the maximum constant arrival rate that a time-varying service process can support with statistical latency guarantees [1]. It acts as a joint mathematical framework, connecting physical layer and link layer, and is used to explore the performance of various wireless networks under certain delay constraint [2]. The concept of effective rate has been widely applied over the last few years to investigate the trade-off among latency, reliability, energy efficiency, and security. Examples can be found in [2], especially in some traditional and future promising applications, including Cellular communication, device-to-device (D2D) communications, peer-to-peer video streaming, visible light communication, full-duplex communications, and ultra-reliable low latency communications (URLLC). The effective rate investigation of these applications are conducted under different fading channel models. In the comprehensive survey paper [2], the authors have summarized that the existing works have investigated the effective rate over Rayleigh [3], Nakagami-m [4], Rician [5], Weibull [6], Gamma [7], $\alpha-\mu$ (equivalently, generalized gamma or Stacy) [8], $\kappa-\mu$ [9], shadowed $\kappa-\mu$ [10], etc., fading channels. More recently, some efforts are devoted to study the effective rate performance over the newly proposed fading channels to cater for different wireless communication scenarios, e.g., [11], Fisher-Snedecor $\mathcal{F}$ for device-to-device communications [12], $\alpha-\eta-\mu$/gamma fading channels [13], two-wave with diffuse-power (TWDP) [14], double shadowed Rician [15], $\alpha-\eta-\kappa-\mu$ fading channels [16].

In [17], [18], a statistical model, namely the mixture gamma (MG) distribution was primarily proposed to provide a more accurate model for the composite shadowing/fading channels compared with the generalized-$\mathcal{K}$ ($\mathcal{K}_G$), the $\mathcal{G}$, and the gamma distributions, besides, it also offers a solution for the closed-form performance metrics for the fading models, where special functions are contained. In [19], the mixture of Gaussian (MoG) distribution was proposed to approximate any arbitrarily shaped non-Gaussian density, e.g., Rayleigh/Log-Normal (RL), Nakagami/Log-Normal (NL), $\kappa-\mu$, $\eta-\mu$, and shadowed $\kappa-\mu$ wireless channels. Both the MG and MoG distributions are possible solutions to accurately approximate the exact distributions. In addition to this, the Fox's H-function distribution is another unified and general approach, which can be used to largely elaborate various fading models, e.g., $\alpha-\mu$, Fisher-Snedecor $\mathcal{F}$, $\mathcal{K}_G$, and extended generalized-K (EGK) [20], [21].

In order to provide a generic framework for the effective rate analysis over various fading channels, it is a high necessity to explore the feasibility of either applying the highly accurate MG and MoG approaches or the exact powerful Fox's H-function approach on the effective rate analysis. For instance, the MG method was used in [22] to model the received instantaneous signal-to-noise ratio (SNR), facilitating the analysis of secrecy metrics. Besides, the authors in [13] used the MG and MoG distributions to assist the effective rate analysis over the composite $\alpha-\eta-\mu$/gamma fading channels. To the authors' best knowledge, no work has so far investigated the effects of using the MG, MoG, and Fox's H-function over various fading channel models on the investigation of effective rate analysis.

To this end, the core of interest in this paper is to showcase the effective rate analysis over wireless channels with the assistance of the MG, MoG, and Fox's H-function distributions. The contributions and insights of this paper are

- √ Three closed-form effective rate expressions are correspondingly derived with the aid of the MG, MoG, and Fox's H-function distributions, they are given in terms of the Fox's H-function. Besides, a highly accurate approximated MoG-based effective rate expression is also presented. The accuracy of all analytical results are examined via the Monte-Carlo simulations.
- √ The insights obtained herein are three-fold
  - The effective rate representations with the MG and MoG distributions are given in terms of univariate Merjer's G-function and bivariate Fox's H-function, respectively. From the numerical evaluation perspective, the MG approach is more accessible and outperforms the MoG approach.
  - The MoG solution illustrates its advantage when the PDF of wireless channels are not exactly known. Though seemingly having a complex effective rate expression, the approximated effective rate representation address this concern, and offers a simple but highly accurate approximation to the MoG solution.
  - If the received SNR could be re-expressed in terms of the Fox's H-function distribution, then the Fox's H-function based approach enjoys highly preference compared to MG and MoG methods due to its exact representation. Nevertheless, the MG and MoG approach are relatively beneficial.

Mathematical Functions and Notations: $j \triangleq \sqrt{-1}$, $\Gamma(.)$ is the complete Gamma function, $H_{p,q}^{m,n}[\cdot]$ is the univariate Fox's H-function [23, Eq. (1.2)], $H_{p,q;p_1,q_1;p_2,q_2}^{m,n;m_1,n_1;m_2,n_2}[\cdot]$ is the extended generalized bivariate Fox's H-function [23, Eq. (2.56)]. ${}_1F_1(a;b;x)$ is the Confluent hypergeometric function [24, Eq. (9.210)]. $\mathcal{M}[f(x),s] = \int_0^\infty f(x)x^{s-1}dx$ denotes the Mellin transform of $f(x)$ [23, Eq. (2.1)].

II. Problem Formulation and Preliminary

A. problem formulation

The normalized effective rate over the instantaneous received SNR $\gamma, \gamma \geq 0$ with the average SNR $\bar{\gamma}$ is defined as [25]

$$\mathcal{R} = -\frac{1}{A}\log_2\left[\underbrace{\mathcal{E}\left((1+\gamma)^{-A}\right)}_{\mathcal{U}}\right] \text{ bits/s/Hz}, \tag{1}$$

where $A = \frac{\theta TB}{\ln 2}$. θ is the delay quality of service (QoS) exponent, T is the block-length, and B denotes the bandwidth of the system. $\mathcal{E}$ denotes the expectation operator.

As stated in the Introduction, the MG, MoG, and Fox's H-function distributions are general tools to model the instantaneous received SNR γ. The former two distributions are highly approximated solutions, while the latter one is an exact representation.

B. Preliminary

1) MG distribution: According to [17], for the known fading channel characteristics, the instantaneous received SNR can be rewritten as follows with the assistance of MG distribution

$$f(\gamma) = \sum_{l=1}^{L} \alpha_l \gamma^{\beta_l - 1}\exp(-\zeta_l\gamma), \tag{2}$$

where L is the number of terms, and $\alpha_l, \beta_l, \zeta_l$ are the parameters of the lth gamma component.

2) MoG distribution: On the basis of the unsupervised EM learning algorithm, the MoG distribution is essentially beneficial when the characteristics of fading channels is unavailable. γ can be modeled as [19]:

$$f(\gamma) = \sum_{l=1}^{C} \frac{w_l}{\sqrt{8\pi\bar{\gamma}}\eta_l\sqrt{\gamma}}\exp\left(-\frac{(\sqrt{\gamma/\bar{\gamma}} - \mu_l)^2}{2\eta_l^2}\right), \tag{3}$$

where C represents the number of Gaussian components. $w_l > 0$, μ_l, and η_l are the lth weight, mean, and variance with the constraint of $\sum_l^C w_l = 1$.

3) Fox's H-function distribution: For the known fading characteristics, the Fox's H-function distribution is another general and flexible tool to model the received SNR [21].

$$\begin{aligned} f(\gamma) &= \kappa H_{p,q}^{m,n}\left[\lambda\gamma \middle| \begin{matrix}(a_i, A_i)_{i=1:p} \\ (b_l, B_l)_{l=1:q}\end{matrix}\right] \\ &\overset{(a)}{=} \frac{\kappa}{2\pi j}\int_{\mathcal{L}} \frac{\prod_{l=1}^{m}\Gamma(b_l + B_l s)\prod_{i=1}^{n}\Gamma(1-a_i-A_i s)(\lambda\gamma)^{-s}}{\prod_{l=m+1}^{q}\Gamma(1-b_l-B_l s)\prod_{i=n+1}^{p}\Gamma(a_i + A_i s)}ds, \end{aligned} \tag{4}$$

where $\lambda > 0$ and κ are constants such that $\int_0^\infty f_k(\gamma_k)d\gamma_k = 1$. $A_i > 0$ for all $i = 1, \cdots, p$, and $B_l > 0$ for all $l = 1, \cdots, q$. $0 \leq m \leq q$, $0 \leq n \leq p$, $\mathcal{L}$ is a suitable contour separating the poles of the gamma functions $\Gamma(b_l + B_l s)$ from the poles of the gamma functions $\Gamma(1 - a_i - A_i s)$. Step (a) is developed by expressing the Fox's H-function in terms of its definition.

III. Effective Rate Characteristics

Theorem 1. *Using the MG, MoG, and Fox's H-function distributions, the effective rate over wireless channels are respectively given by (5) in terms of Meijer's G-function*[1]*, (6) in terms of bivariate Fox's H-function*[2]*, and (7) in terms of univariate Fox's H-function*[3]*, which are shown at the top of next page,*

$$\mathcal{R}_{MG} = -\frac{1}{A}\log_2\left[\sum_{l=1}^{L}\frac{\alpha_l}{\zeta_l^{\beta_l}\Gamma(A)}G_{2,1}^{1,2}\left[\frac{1}{\zeta_l}\middle|\begin{matrix}1-\beta_l, 1-A \\ 0\end{matrix}\right]\right], \tag{5}$$

[1]It is noted that the implementation of the Meijer G-function is already available at MATHEMATICA, MATLAB, and MAPLE.

[2]It is noted that the bivariate Fox's H-function is computable and programmable in the open literature [26], [27]

[3]The numerical evaluation of the univariate Fox's H-function is based on the method proposed in [28, Appendix. A].

$$\mathcal{R}_{MoG} = -\frac{1}{A}\log_2\left[\sum_{l=1}^{C}\frac{w_l\Gamma(\frac{1}{2})}{\sqrt{\pi}\Gamma(A)}H_{1,0:2,0:1,1}^{0,1:0,1:1,1}\left[\frac{2\eta_l^2}{\mu_l^2},\frac{1}{2\bar{\gamma}\eta_l^2}\middle|\begin{matrix}(1,-1,1)\\-\end{matrix}\middle|\begin{matrix}(1,1),(\frac{1}{2},1)\\-\end{matrix}\middle|\begin{matrix}(\frac{3}{2},1)\\(A,1)\end{matrix}\right]\right], \tag{6}$$

$$\mathcal{R}_{Fox} = -\frac{1}{A}\log_2\left[\frac{\kappa}{\Gamma(A)}H_{p+1,q+1}^{m+1,n+1}\left[\lambda\middle|\begin{matrix}(a_n,A_n),(0,1),(a_{n+1},A_{n+1}),\cdots,(a_p,A_p)\\(b_m,B_m),(A-1,1),(b_{m+1},B_{m+1}),\cdots,(b_p,B_q)\end{matrix}\right]\right]. \tag{7}$$

Proof. Re-expressing $(1+\gamma)^{-A}$ in terms of the Meijer's G-function [29, Eq.(8.4.2.5)]

$$\begin{aligned}(1+\gamma)^{-A} &= \frac{1}{\Gamma(A)}G_{1,1}^{1,1}\left[\gamma\middle|\begin{matrix}1-A\\0\end{matrix}\right]\\ &= \frac{1}{\Gamma(A)}H_{1,1}^{1,1}\left[\gamma\middle|\begin{matrix}(1-A,1)\\(0,1)\end{matrix}\right],\end{aligned} \tag{8}$$

and then plugging it with (2) into $\mathcal{U}$ given in (1), yields

$$\begin{aligned}\mathcal{U} &= \sum_{l=1}^{L}\frac{\alpha_l}{\Gamma(A)}\int_0^\infty\frac{\exp(-\zeta_l\gamma)}{\gamma^{1-\beta_l}}G_{1,1}^{1,1}\left[\gamma\middle|\begin{matrix}1-A\\0\end{matrix}\right]d\gamma\\ &= \sum_{l=1}^{L}\frac{\alpha_l}{\zeta_l^{\beta_l}\Gamma(A)}G_{2,1}^{1,2}\left[\frac{1}{\zeta_l}\middle|\begin{matrix}1-\beta_l,1-A\\0\end{matrix}\right],\end{aligned} \tag{9}$$

then with the help of [29, Eqs.(2.25.2.3) and (8.3.2.21)], the proof is achieved.

Similarly, the proof for (6) starts with the substitution of (3) into $\mathcal{U}$,

$$\mathcal{U} = \sum_{l=1}^{C}w_l\underbrace{\int_0^\infty\frac{1}{(1+\gamma)^A}\overbrace{\frac{\gamma^{-1/2}}{\sqrt{8\pi\bar{\gamma}\eta_l}}\exp\left(-\frac{(\gamma-\bar{\gamma}\mu_l)^2}{2\bar{\gamma}^2\eta_l^2}\right)}^{g(\gamma)}d\gamma}_{\mathcal{U}_1}. \tag{10}$$

Next utilizing Parseval's relation for Mellin transform [30, Eq. (8.3.23)], $\mathcal{U}_1$ could be rewritten as

$$\mathcal{U}_1 = \frac{1}{2\pi j}\int_{\mathcal{L}}\mathcal{M}\left[g(\gamma),1-s\right]\mathcal{M}[(1+\gamma)^{-A},s]ds, \tag{11}$$

applying the results of [19, Eq. (40)] and [29, Eq.(8.4.2.5)] into (11), $\mathcal{M}\left[g(\gamma),1-s\right]$ and $\mathcal{M}[(1+\gamma)^{-A},s]$ are respectively given by

$$\mathcal{M}\left[g(\gamma),1-s\right] = \frac{\Gamma(\frac{1}{2}-s)}{\sqrt{\pi}(2\bar{\gamma}\eta_l^2)^s}{}_1F_1\left[s,\frac{1}{2},-\frac{\mu_l^2}{2\eta_l^2}\right], \tag{12a}$$

$$\mathcal{M}[(1+\gamma)^{-A},s] = \frac{\Gamma(s)\Gamma(A-s)}{\Gamma(A)}. \tag{12b}$$

Next, substituting (12a) and (12b) into $\mathcal{U}_1$, then representing the Confluent hypergeometric function in terms of Meijer's G-function [29, Eq.(8.4.45.1)]

$${}_1F_1[a;b;-x] = \frac{\Gamma(b)}{\Gamma(a)}G_{1,2}^{1,1}\left[x\middle|\begin{matrix}1-a\\0,1-b\end{matrix}\right],$$

and re-expressing the Meijer's G-function in terms of the Mellin–Barnes integral, yields

$$\begin{aligned}\mathcal{U}_1 =& \frac{-\Gamma(\frac{1}{2})}{4\pi^2\sqrt{\pi}\Gamma(A)}\int_{\mathcal{L}}\int_{\mathcal{L}_1}\frac{\Gamma(s-\xi)\Gamma(\xi)}{\Gamma(\frac{1}{2}-\xi)}\left(\frac{2\eta_l^2}{\mu_l^2}\right)^\xi\\ &\times\Gamma(A-s)\Gamma\left(s-1/2\right)\left(\frac{1}{2\bar{\gamma}\eta_l^2}\right)^s dsd\xi.\end{aligned} \tag{13}$$

Finally, applying the definition of bivariate Fox's H-function [23, Appendix A.1] and making some mathematical manipulations, the proof for (6) is achieved.

Similarly, the proof for (7) is accomplished by using (8) and the Mellin transform of the product of two Fox's H-functions [29, Eq. (25.2.1.1)]. ■

Remark 1. *Since the instantaneous SNR can be re-expressed in terms of the sum of C normally distributed random variables, i.e., $\gamma = \sum_{l=1}^{C}\gamma_l$, and $\gamma_l \sim \mathcal{N}(\mu_l,\eta_l)$, then $\mathcal{R}_{MoG}$ can be approximated as (14), shown at the top of next page.*

Proof. Revisiting $\mathcal{U}$ in (1), and making change of variables $\sqrt{\frac{\gamma}{\bar{\gamma}}} = y$, yields

$$\mathcal{U} = \sum_{l=1}^{C}w_l\int_0^\infty\frac{(1+\bar{\gamma}y^2)^{-A}}{\sqrt{2\pi}\eta_l}\exp\left(-\frac{(y-\mu_l)^2}{2\eta_l^2}\right)dy, \tag{15}$$

subsequently applying the result given in [31, Eq. (4)], the proof is finished. ■

IV. Numerical Results

In order to validate the tightness of (5) and (6), and the accuracy of (7), the Monte-Carlo simulations are thereafter conducted. The usefulness of the MG approach is examined by considering the $\mathcal{K}_G$ distribution. The comparison of the effective rate between the MG and MoG solutions is performed over the $\kappa-\mu$ ($\kappa=3,\mu=1$, equivalently, Rician) fading channel, where the MG-based parameters used to model $\mathcal{K}_G$ and $\kappa-\mu$ are shown in Table. I. The MoG-based parameters to model the $\kappa-\mu$ and $\eta-\mu$ fading channels are from [19, Tables. IV, VI, and VII].

Fig. 1 plots the $\mathcal{R}_{MG}$ against $\bar{\gamma}$ for selected values of m, larger shaping factor m results in higher effective rate performance. Fig. 2 plots our analytical effective rate expressions given in (5) and (6) over $\kappa-\mu$ fading channels. The performance curves for the effective rate metric, based on the simulated results and the MG and MoG expressions, demonstrates an excellent match. One can also observe that the effective rate performance degrades as the increase of A.

$$\mathcal{R}_{MoG} \approx -\frac{1}{A}\log_2\left[\sum_{l=1}^{C} w_l \left(\frac{2}{3(1+\bar{\gamma}\mu_l^2)^A} + \frac{1}{6(1+\bar{\gamma}(\mu_l+\sqrt{3}\eta_l)^2)^A} + \frac{1}{6(1+\bar{\gamma}(\mu_l-\sqrt{3}\eta_l)^2)^A}\right)\right]. \quad (14)$$

TABLE I: Simulations parameters for the MG distribution

Distribution	**Parameters**, $\alpha_l = \frac{\theta_l}{\sum_{k=1}^{L_i} \theta_k \Gamma(\beta_k)\zeta_k^{-\beta_k}}$, $\bar{\gamma}_i$ is the average SNR.
$\mathcal{K}_G$ [17, Sec. III.B], m and k are distribution shaping parameters, $L = 5$.	$\beta_l = m$, $\zeta_l = \frac{\lambda}{t_l}$, $\lambda = \frac{km}{\bar{\gamma}}$, $\theta_l = \frac{\lambda^m w_l t_l^{k-m-1}}{\Gamma(m)\Gamma(k)}$, t_l, w_l are the abscissas and weight factors for the Gaussian-Laguerre integration [32, Table 25.9].
$\kappa-\mu(\mu=1)$ [17, Sec. III.F], $0 \leq n < \infty$, $L = 20$	$\beta_l = l$, $\zeta_l = \frac{(1+\kappa)}{\bar{\gamma}}$, $\theta_l = \frac{(1+\kappa)}{\exp(\kappa)[(l-1)!]^2\bar{\gamma}}\left(\frac{\kappa(1+\kappa)}{\bar{\gamma}}\right)^{l-1}$.

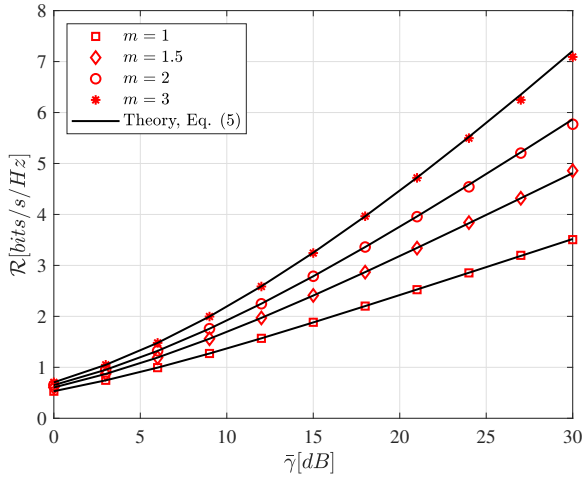

Fig. 1: $\mathcal{R}_{MG}$ versus $\bar{\gamma}$ over $\mathcal{K}_G$ fading channels for selected values of m when $k = 4$ and $A = 3$.

Fig. 3 compares the results given in (6) and (14) over the $\eta-\mu$ fading channels for two scenarios: Format I ($0 < \eta < \infty$) and Format II ($-1 < \eta < 1$). One can conclude that (i) the approximated MoG-based effective rate expression provides a highly accurate and simple approach to the MoG-based expression; and (ii) the impact of the increase of A on the effective rate metric is smaller for the Format I $\eta-\mu$ fading channels compared to the Format II.

In Fig. 4, the effective rate over $\alpha-\mu$ (including Rayleigh, Nakagami-m, Weibull, etc.) [21, Table. I], Fisher-Snedecor $\mathcal{F}$, and EGK fading channels are presented. One can observe that (i) the analytical result given in (7) is in perfect match with the Monte-Carlo simulation; and (ii) comparing $\mathcal{R}_{Fox}$ over Rayleigh ($\alpha = 2, \mu = 1$) fading channel with that over Nakagami-m ($\alpha = 2, \mu = m = 4$) and Weibull ($\alpha = 3, \mu = 1$) fading channel, one can conclude that an increase of shaping parameters α and μ results in the increase of effective rate, in

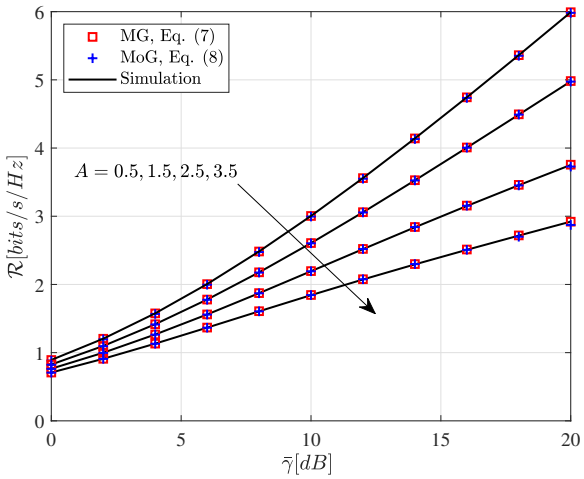

Fig. 2: Effective rate $\mathcal{R}_{MG}$ and $\mathcal{R}_{MoG}$ against $\bar{\gamma}$ over $\kappa-\mu$ fading channels when $\kappa = 3$ and $\mu = 1$.

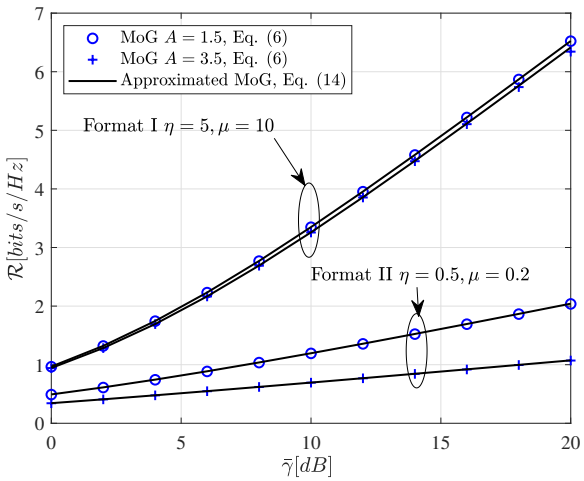

Fig. 3: Effective rate $\mathcal{R}_{MoG}$ against $\bar{\gamma}$ over $\eta-\mu$ fading channels.

other words, the channels with smaller shaping parameters α and μ contribute less to the effective rate.

V. Conclusion

This paper first investigated the effective rate performance of wireless channels, by modeling the received SNRs as the MG, MoG, and Fox's H-function distributed RVs. Closed-form expressions are respectively derived in terms of the Fox's H-function. The analytical results were further examined with the Monte-Carlo simulations. One can conclude that (i) the MG approach provides the most simplest form; (ii) the Fox's

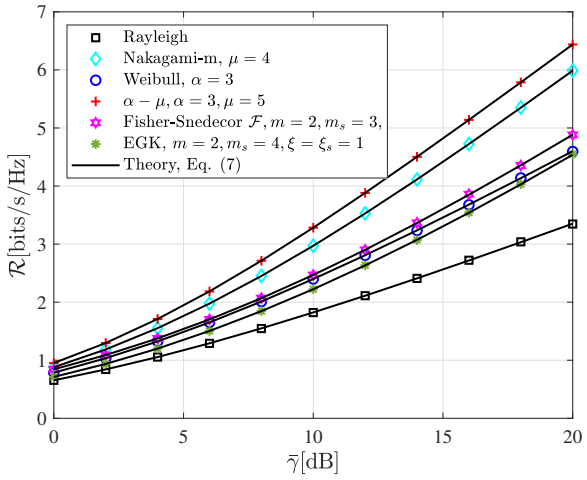

Fig. 4: $\mathcal{R}_{Fox}$ versus $\bar{\gamma}$ over Rayleigh, Nakagami-m, Weibull, $\alpha - \mu$, Fisher-Snedecor $\mathcal{F}$, and EGK fading channels when $A = 2$.

H-function approach provides a unified, exact and general tool to evaluate the effective rate performance if the received SNR can be rewritten in the manner of Fox's H-function distributed RV; and (iii) the effective rate expressions with MG and MoG are accurately approximated compared with the Fox's H-function solution.

ACKNOWLEDGMENT

This work has been supported by the Luxembourg National Research Fund (FNR) project, titled Exploiting Interference for Physical Layer Security in 5G Networks (CIPHY).

REFERENCES

[1] Dapeng Wu and R. Negi, "Effective capacity: a wireless link model for support of quality of service," *IEEE Trans. Wireless Commun.*, vol. 2, no. 4, pp. 630–643, July 2003.

[2] M. Amjad, L. Musavian, and M. H. Rehmani, "Effective capacity in wireless networks: A comprehensive survey," *IEEE Commun. Surveys Tuts.*, vol. 21, no. 4, pp. 3007–3038, 2019.

[3] M. C. Gursoy, D. Qiao, and S. Velipasalar, "Analysis of energy efficiency in fading channels under QoS constraints," *IEEE Trans. Wireless Commun.*, vol. 8, no. 8, pp. 4252–4263, Aug. 2009.

[4] K. P. Peppas, P. T. Mathiopoulos, and J. Yang, "On the effective capacity of amplify-and-forward multihop transmission over arbitrary and correlated fading channels," *IEEE Wireless Commun. Lett.*, vol. 5, no. 3, pp. 248–251, Jun. 2016.

[5] U. Celentano and S. Glisic, "Effective capacity of imperfect adaptive wireless communication systems," in *IEEE PIMRC*, vol. 4, Berlin, Germany, 2005, pp. 2191–2195 Vol. 4.

[6] M. You, H. Sun, J. Jiang, and J. Zhang, "Effective rate analysis in Weibull fading channels," *IEEE Wireless Commun. Lett.*, vol. 5, no. 4, pp. 340–343, Aug. 2016.

[7] M. Z. Hassan, V. C. M. Leung, M. J. Hossain, and J. Cheng, "Effective capacity performance of coherent POLMUX OWC with power adaptation," in *IEEE GLOBECOM*, San Diego, CA, USA, 2015, pp. 1–7.

[8] J. Zhang, L. Dai, Z. Wang, D. W. K. Ng, and W. H. Gerstacker, "Effective rate analysis of MISO systems over $\alpha - \mu$ fading channels," in *Proc. IEEE Glob. Commun. Conf. (GLOBECOM)*, Dec 2015, pp. 1–6.

[9] J. Zhang, Z. Tan, H. Wang, Q. Huang, and L. Hanzo, "The effective throughput of MISO systems over κ –μ fading channels," *IEEE Trans. Veh. Technol.*, vol. 63, no. 2, pp. 943–947, Feb. 2014.

[10] J. Zhang, L. Dai, W. H. Gerstacker, and Z. Wang, "Effective capacity of communication systems over $\kappa - \mu$ shadowed fading channels," *Electronics Letters*, vol. 51, no. 19, pp. 1540–1542, 2015.

[11] M. Matthaiou, G. C. Alexandropoulos, H. Q. Ngo, and E. G. Larsson, "Analytic framework for the effective rate of MISO fading channels," *IEEE Trans. Commun.*, vol. 60, no. 6, pp. 1741–1751, Jun. 2012.

[12] F. S. Almehmadi and O. S. Badarneh, "On the effective capacity of Fisher–Snedecor $\mathcal{F}$ fading channels," *Electron. Lett.*, vol. 54, no. 18, pp. 1068–1070, 2018.

[13] H. Al-Hmood and H. S. Al-Raweshidy, "Unified approaches based effective capacity analysis over composite $\alpha - \eta - \mu$/gamma fading channels," *Electron. Lett.*, vol. 54, no. 13, pp. 852–853, 2018.

[14] H. Kaur, V. Kansal, and S. Singh, "Effective rate analysis of two-wave with diffuse-power fading channels," *IET Commun.*, vol. 13, no. 3, pp. 339–344, 2019.

[15] R. Singh, M. Rawat, and P. M. Pradhan, "Effective capacity of wireless networks over double shadowed Rician fading channels," *Wireless Networks*, vol. 26, no. 2, pp. 1347–1355, 2020.

[16] Y. Ai, A. Mathur, L. Kong, and M. Cheffena, "Effective throughput analysis of $\alpha - \eta - \kappa - \mu$ fading channels," *IEEE Access*, vol. 8, pp. 57 363–57 371, 2020.

[17] S. Atapattu, C. Tellambura, and H. Jiang, "A mixture gamma distribution to model the SNR of wireless channels," *IEEE Trans. Wireless Commun.*, vol. 10, no. 12, pp. 4193–4203, Dec. 2011.

[18] H. Al-Hmood and H. S. Al-Raweshidy, "Unified modeling of composite $\kappa - \mu$/gamma, $\eta - \mu$/gamma, and $\alpha - \mu$/gamma fading channels using a mixture gamma distribution with applications to energy detection," *IEEE Antennas Wireless Propag. Lett*, vol. 16, pp. 104–108, 2017.

[19] B. Selim, O. Alhussein, S. Muhaidat, G. K. Karagiannidis, and J. Liang, "Modeling and analysis of wireless channels via the mixture of gaussian distribution," *IEEE Trans. Veh. Technol.*, vol. 65, no. 10, pp. 8309–8321, Oct. 2016.

[20] Y. A. Rahama, M. H. Ismail, and M. Hassan, "On the sum of independent Fox's H-function variates with applications," *IEEE Trans. Veh. Technol.*, vol. 67, no. 8, pp. 6752–6760, Aug. 2018.

[21] L. Kong, G. Kaddoum, and H. Chergui, "On physical layer security over Fox's H-function wiretap fading channels," *IEEE Trans. Veh. Technol.*, vol. 68, no. 7, pp. 6608–6621, Jul. 2019.

[22] L. Kong and G. Kaddoum, "Secrecy characteristics with assistance of mixture gamma distribution," *IEEE Wireless Commun. Lett.*, vol. 8, no. 4, pp. 1086–1089, Aug. 2019.

[23] A. M. Mathai, R. K. Saxena, and H. J. Haubold, *The H-function: theory and applications*. Springer Science & Business Media, 2009.

[24] I. S. Gradshteyn and I. M. Ryzhik, *Table of integrals, series, and products*. Academic press, 2014.

[25] C. Zhong, T. Ratnarajah, K. . Wong, and M. . Alouini, "Effective capacity of multiple antenna channels: correlation and keyhole," *IET Commun.*, vol. 6, no. 12, pp. 1757–1768, Aug. 2012.

[26] K. P. Peppas, "A new formula for the average bit error probability of dual-hop amplify-and-forward relaying systems over generalized shadowed fading channels," *IEEE Wireless Commun. Lett.*, vol. 1, no. 2, pp. 85–88, Apr. 2012.

[27] H. Chergui, M. Benjillali, and M. Alouini, "Rician K -factor-based analysis of XLOS service probability in 5G outdoor ultra-dense networks," *IEEE Wireless Commun. Lett.*, vol. 8, no. 2, pp. 428–431, Apr. 2019.

[28] K. P. Peppas, F. Lazarakis, A. Alexandridis, and K. Dangakis, "Simple, accurate formula for the average bit error probability of multiple-input multiple-output free-space optical links over negative exponential turbulence channels," *Optics lett.*, vol. 37, no. 15, pp. 3243–3245, 2012.

[29] A. P. Prudnikov, Y. A. Brychkov, and O. I. Marichev, *Integrals and Series: More special functions*. Gordon and Breach Science Publishers, 1990, vol. 3.

[30] L. Debnath and D. Bhatta, *Integral transforms and their applications*. CRC press, 2014.

[31] G. Pan, C. Tang, X. Zhang, T. Li, Y. Weng, and Y. Chen, "Physical-layer security over non-small-scale fading channels," *IEEE Trans. Veh. Technol.*, vol. 65, no. 3, pp. 1326–1339, Mar. 2016.

[32] M. Abramowitz and I. A. Stegun, *Handbook of mathematical functions: with formulas, graphs, and mathematical tables*. Courier Corporation, 1965, vol. 55.